Ultrashort pulse generation from 156 μm mode-locked VECSEL at room temperature

Aghiad Khadour, Sophie Bouchoule, Guy Aubin, Jean-Christophe Harmand, Jean Decobert, Jean-Louis Oudar

▶ **To cite this version:**

Aghiad Khadour, Sophie Bouchoule, Guy Aubin, Jean-Christophe Harmand, Jean Decobert, et al.. Ultrashort pulse generation from 156 μm mode-locked VECSEL at room temperature. Optics Express, 2010, 18 (19), pp.19902. 10.1364/OE.18.019902 . hal-04433540

HAL Id: hal-04433540
https://hal.science/hal-04433540

Submitted on 2 Feb 2024

HAL is a multi-disciplinary open access archive for the deposit and dissemination of scientific research documents, whether they are published or not. The documents may come from teaching and research institutions in France or abroad, or from public or private research centers.

L'archive ouverte pluridisciplinaire **HAL**, est destinée au dépôt et à la diffusion de documents scientifiques de niveau recherche, publiés ou non, émanant des établissements d'enseignement et de recherche français ou étrangers, des laboratoires publics ou privés.

Distributed under a Creative Commons Attribution - NonCommercial - ShareAlike 4.0 International License

Ultrashort pulse generation from 1.56 µm mode-locked VECSEL at room temperature

Aghiad Khadour,[1,*] Sophie Bouchoule,[1] Guy Aubin,[1] Jean-Christophe Harmand,[1] Jean Decobert,[2] and Jean-Louis Oudar[1]

[1]*Laboratoire de Photonique et de Nanostructures, Route de Nozay, 91460 Marcoussis, France*
[2]*Alcatel III-V Lab, Route de Nozay, 91460 Marcoussis, France.*
[*]*aghiad.khadour@polytechnique.edu*

Abstract: We report on a picosecond pulse source delivering near transform-limited pulses in the 1.55 µm wavelength region, based on an optically pumped InP-based mode locked Vertical External Cavity Surface Emitting Laser (VECSEL). The cavity combines two semiconductor elements, a gain structure which includes six strained InGaAlAs quantum wells and a hybrid metal-metamorphic Bragg bottom mirror bonded onto a CVD diamond substrate, and a single quantum well GaInNAs SEmiconductor Saturable Absorber Mirror (SESAM). The laser operates at a repetition frequency of 2 GHz and emits near-transform-limited 1.7 ps pulses with an average output power of 15 mW at room temperature, using 1.7 W pump power at 980nm. The RF line width of the free running laser has been measured to be less than 1 kHz.

©2010 Optical Society of America.

OCIS codes: (140.4050) Mode-locked lasers; (320.7090) Ultrafast lasers; (140.5960) Semiconductor lasers.

References and links

1. M. Kuznetsov, F. Hakimi, R. Sprague, and A. Mooradian, "High-power (<0.5-W CW) diode-pumped vertical-external-cavity surface-emitting semiconductor lasers with circular TEM/sub 00/ beams," IEEE Photon. Technol. Lett. **9**(8), 1063–1065 (1997).
2. M. Kuznetsov, F. Hakimi, R. Sprague, and A. Mooradian, "Design and characteristics of high-power (>0.5-W CW) diode-pumped vertical-external-cavity surface-emitting semiconductor lasers with circular TEM_{00} beams," IEEE J. Sel. Top. Quantum Electron. **5**(3), 561–573 (1999).
3. S. Hoogland, S. Dhanjal, A. C. Tropper, J. S. Roberts, R. Haring, R. Paschotta, F. Morier-Genoud, and U. Keller, "Passively mode-locked diode-pumped surface-emitting semiconductor laser," IEEE Photon. Technol. Lett. **12**(9), 1135–1137 (2000).
4. S. Hoogland, A. Garnache, I. Sagnes, B. Paldus, K. J. Weingarten, R. Grange, M. Haiml, R. Paschotta, U. Keller, and A. C. Tropper, "Picosecond pulse generation with 1.5 µm passively modelocked surface-emitting semiconductor laser," Electron. Lett. **39**(11), 846–847 (2003).
5. H. Lindberg, M. Sadeghi, M. Westlund, S. Wang, A. Larsson, M. Strassner, and S. Marcinkevičius, "Mode locking a 1550 nm semiconductor disk laser by using a GaInNAs saturable absorber," Opt. Lett. **30**(20), 2793–2795 (2005).
6. E. J. Saarinen, J. Puustinen, A. Sirbu, A. Mereuta, A. Caliman, E. Kapon, and O. G. Okhotnikov, "Power-scalable 1.57 microm mode-locked semiconductor disk laser using wafer fusion," Opt. Lett. **34**(20), 3139–3141 (2009).
7. R. Paschotta, R. Haring, A. Garnache, S. Hoogland, A. C. Tropper, and U. Keller, "Soliton-like pulse-shaping mechanism in passively mode-locked surface-emitting semiconductor lasers," Appl. Phys. B **75**(4-5), 445–451 (2002).
8. E. J. Saarinen, R. Herda, and O. G. Okhotnikov, "Dynamics of pulse formation in mode-locked semiconductor disk lasers," J. Opt. Soc. Am. B **24**(11), 2784–2790 (2007).
9. M. Hoffmann, O. D. Sieber, D. J. H. C. Maas, V. J. Wittwer, M. Golling, T. Südmeyer, and U. Keller, "Experimental verification of soliton-like pulse-shaping mechanisms in passively mode-locked VECSELs," Opt. Express **18**(10), 10143–10153 (2010).
10. J. P. Tourrenc, S. Bouchoule, A. Khadour, J. Decobert, A. Miard, J. C. Harmand, and J. L. Oudar, "High power single-longitudinal-mode OP-VECSEL at 1.55 µm with hybrid metal-metamorphic Bragg mirror," Electron. Lett. **43**(14), 754–755 (2007).
11. J.-P. Tourrenc, S. Bouchoule, A. Khadour, J.-C. Harmand, A. Miard, J. Decobert, N. Lagay, X. Lafosse, I. Sagnes, L. Leroy, and J.-L. Oudar, "Thermal optimization of 1.55 µm OP-VECSEL with hybrid metal–metamorphic mirror for single-mode high power operation," Opt. Quantum Electron. **40**(2-4), 155–165 (2008).

#129538 - $15.00 USD Received 3 Jun 2010; revised 3 Aug 2010; accepted 9 Aug 2010; published 3 Sep 2010
(C) 2010 OSA

12. M. L. Dû, J. C. Harmand, O. Mauguin, L. Largeau, L. Travers, and J. L. Oudar, "Quantum-well saturable absorber at 1.55 μm on GaAs substrate with a fast recombination rate," Appl. Phys. Lett. **88**, 201110 (2006).
13. E. D. Palik, ed., *Handbook of Optical Constants of Solids* (Academic Press, San Diego, 1985), Vol. 1.
14. M. Haiml, R. Grange, and U. Keller, "Optical characterization of semiconductor saturable absorbers," Appl. Phys. B **79**(3), 331–339 (2004).
15. D. J. Maas, B. Rudin, A. R. Bellancourt, D. Iwaniuk, S. V. Marchese, T. Südmeyer, and U. Keller, "High precision optical characterization of semiconductor saturable absorber mirrors," Opt. Express **16**(10), 7571–7579 (2008).
16. T. R. Schibli, E. R. Thoen, F. X. Kärtner, and E. P. Ippen, "Suppression of Q-switched mode locking and break-up into multiple pulses by inverse saturable absorption," Appl. Phys. B **70**, S41–S49 (2000).
17. R. Grange, M. Haiml, R. Paschotta, G. J. Spühler, L. Krainer, M. Golling, O. Ostinelli, and U. Keller, "New regime of inverse saturable absorption for self-stabilizing passively mode-locked lasers," Appl. Phys. B **80**, 151–158 (2005).
18. E. Cojocaru, T. Julea, and N. Herisanu, "Stability and astigmatic compensation analysis of five- and six- or seven-mirror cavities for mode-locked dye lasers," Appl. Opt. **28**(13), 2577–2580 (1989).

1. Introduction

The first demonstration of optically pumped VECSEL [1, 2] formed a new step to bridge the gap between semiconductor lasers and solid-state lasers: It combines the versatility of a semiconductor quantum well gain medium with the capacity to operate at high average power with a diffraction limited output beam. Semiconductor lasers typically have a broad gain bandwidth, theoretically capable of supporting ultrashort pulses.

The requirements of gigahertz repetition rate pulsed lasers is rapidly growing for applications in high-energy physics, optical testing of semiconductor electronics and telecommunication components, in optical clocking of integrated circuits, and in optoelectronic performance enhancements of analog-to-digital converters. The low jitter multi-gigahertz pulse sources to date have involved either an edge-emitting semiconductor laser, which is usually actively or hybridly mode locked, or a harmonically mode locked fiber ring laser. A particularly interesting application of VECSELs is in high power ultrashort pulse generation at high repetition rates. Both synchronously pumped lasers and passively mode-locked systems have been studied. The most stable and common technique, for ultrashort laser pulse generation, is utilizing a semiconductor saturable absorber mirror (SESAM) as a mode-locking element. After the first demonstration of passive mode locked VECSEL in 2000 using a SESAM [3], a period of rapid progress followed during which the great flexibility in design and fabrication of the semiconductor gain structure and absorber was exploited to reach sub picosecond pulse durations. Most of this early work was done at different repetition rates in the 1 μm spectral region, with a GaAs-based material. Progress towards ultrashort pulse generation at 1.55 μm window at room temperature, was till now very difficult because of the poor thermal behavior of quaternary InP-based semiconductor compounds [4–6].

The physical mechanism for ultrashort pulse generation in passively mode-locked VECSELs, is rather complex as two semiconductor structures are employed, a gain structure and a SESAM structure [7–9]. Both structures have optical properties that depend on wavelength, temperature and carrier density. The performance of the mode locked VECSEL for a given application depends on both the detailed design of both structures, and on the properties of the laser cavity.

In this paper, we present a gain structure optimized for: low thermal impedance and more pump power absorption, so as to obtain a high output power at room temperature. We have already reported single-longitudinal-mode operation thanks to the insertion inside the cavity of a glass etalon [10]. For mode-locked operation, the different macroscopic parameters of SESAM structures were characterized and the best structure selected for mode-locked operation. Using the two optimized structures in a Z-cavity led to mode locked regime at room temperature. The evolution of the pulse characteristics from the onset of mode-locking to a true mode-locked steady state was studied by varying the intracavity spot size ratio on the gain and saturable absorber mirrors. A near transform limited short pulse emission with a RF linewidth of less than 1 kHz for the free running laser was measured.

#129538 - $15.00 USD Received 3 Jun 2010; revised 3 Aug 2010; accepted 9 Aug 2010; published 3 Sep 2010
(C) 2010 OSA

2. VECSEL structure and continuous performance

The gain structure (hereafter called ½ VCSEL) design consists of a simple Bragg mirror, with a series of quantum wells (QWs) ordered into a resonant periodic gain structure, on a substrate of high thermal conductivity. We have demonstrated high power CW RT operation of an optically-pumped 1.55 µm VECSEL using a thermally optimized ½-VCSEL chip, using a hybrid metal-metamorphic GaAs/AlAs mirror and bonded on a SiC substrate, and showed that due to the good thermal conductivity of the metal-metamorphic mirror, the use of a CVD diamond host substrate instead of the SiC substrate can further improve the thermal resistance of the ½-VCSEL chip [11]. We present here the details of the ½ VCSEL structure.

1.1 VECSEL structure details

The InP-based gain structure with 2λ-thick active region, grown in reverse order by metal-organic vapor-phase epitaxy includes the six strained InGaAlAs quantum wells, distributed among three optical standing-wave anti-node positions with a 2-2-2 distribution. Molecular beam epitaxy (MBE) regrowth is then used to form a 17-pair metamorphic GaAs/$Al_{0.95}$GaAs semiconductor Bragg mirror, whose reflectivity is enhanced thanks to the deposition of a 150 nm-thick Au layer, and is calculated to be greater than 99.9% at 1550 nm. The overall structure is then mounted onto a high thermal conductivity CVD-diamond substrate thanks to an $AuIn_2$ eutectic bonding. After removal of the InP-substrate and of the etch–stop layer, a quarter-wavelength $SiON_x$ anti-reflecting (AR) layer at 980 nm (wavelength of the laser diode pump, for angle of pump 45°) is deposited on the sample surface. The thickness of the top InP layer acting as a phase layer is precisely etched, so that the position of the resonant half-cavity mode is close to the gain maximum after the AR layer deposition.

The details of the structure is shown on Fig. 1(a), and its reflectivity spectrum measured by Fourier transformed infra-red spectroscopy in Fig. 1(b), where the half cavity resonance is close to the 1.55 µm design wavelength. The theoretical calculated group-delay dispersion (GDD) is shown on figue1(c), the GDD has a decreasing positive values below $4 \cdot 10^3$ fs^2 after the 1.55µm. The generation of ultrashort pulses requires a minimum overall GDD, so we should compensate the GDD of the ½ VCSEL by using a SESAM with negative GDD.

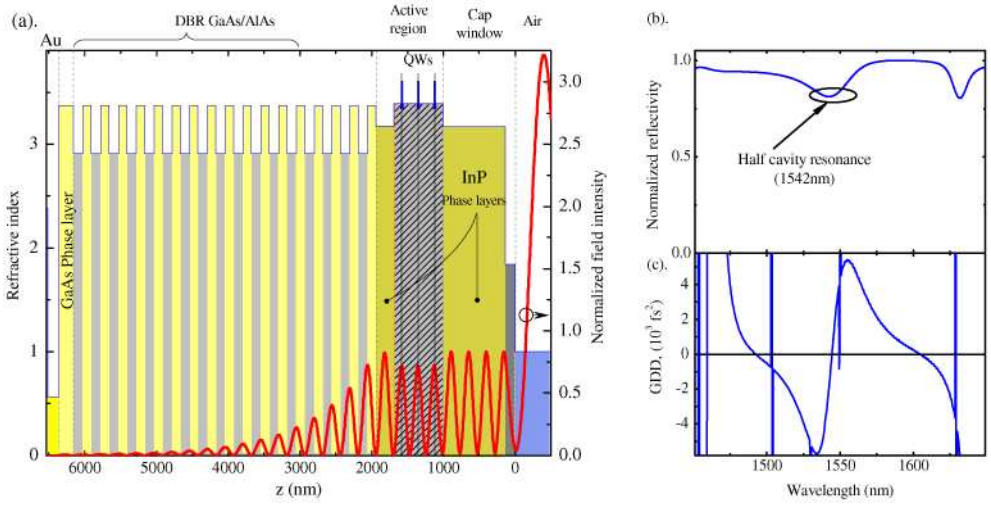

Fig. 1. (a). The layout of the gain structure presents the refractive index structure (bleu), and calculated standing wave intensity pattern for λ=1550 nm (red), (b). Typical measured reflectivity spectrum of the gain structure at room temperature. (c). Calculated GDD.

1.2 VECSEL performance

The ½-VCSEL chip was first included in a plane-concave cavity (concave dielectric mirror, R=99%, Roc=25 mm) for the evaluation of its CW performance at room temperature (RT)

#129538 - $15.00 USD Received 3 Jun 2010; revised 3 Aug 2010; accepted 9 Aug 2010; published 3 Sep 2010
(C) 2010 OSA

under optical pumping, with a cavity length of ~20 mm, as shown in Fig. 2. The temperature was stabilized using a Peltier element and Cu back plate with a water flow for temperature below 15°C. The water flow was switched off for higher heatsink temperatures.

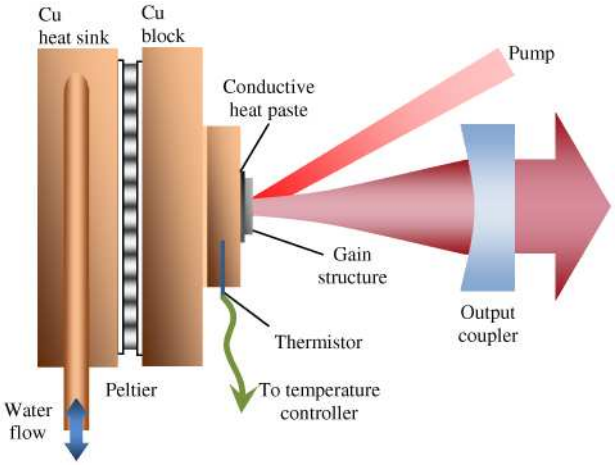

Fig. 2. VECSEL cavity setup. The gain sample is bonded to the copper mount with a heat conductive paste, this is in turn attached to the copper block which is temperature controlled by a Peltier device. The back plate of the device can be water-cooled for temperatures below 15°C.

These tests have also been used to identify the optimum position of the resonant half-cavity mode leading to the lowest threshold and highest optical output power. A continuous-wave (CW) lasing operation was obtained using a large area multimode pump laser diode (~60μm).

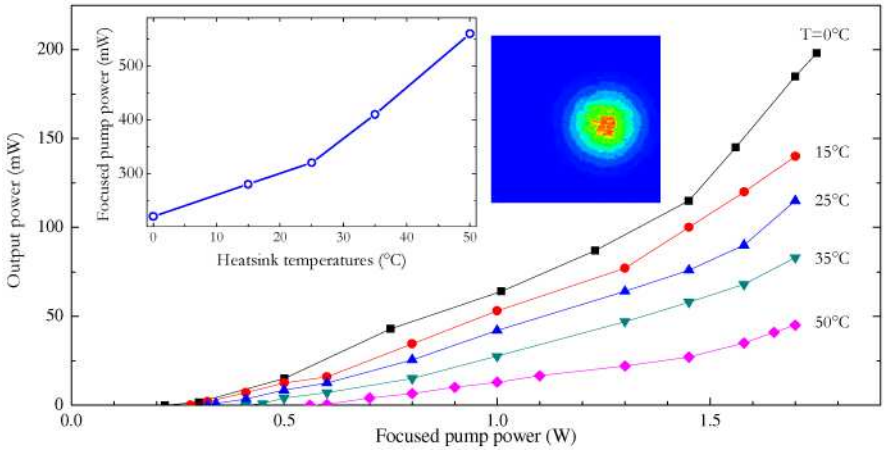

Fig. 3. Continuous-wave emitted power versus incident pump power at different temperatures, in the plane-concave cavity configuration, using a 99% HR dielectric mirror. Water cooling of the heat sink was used for T ≤ 15°C, while a TE cooler alone (no water flow) was sufficient above 15°C. The insets show: the threshold pump power as a function of heatsink temperature, and output beam profile measured with a CCD camera at the output power of 120 mW at room temperature.

The central issue for obtaining high average output power in single-transverse mode operation is to match the laser mode size on the gain structure to the pump spot. Figure 3 reports the results of the output power as a function of the pump power, with lasing up to 50°C (Peltier controller limitation) with maximum output power of 40mW, without rollover. The maximum output cw power at room temperature was > 120 mW (TEM_{00} emission: inset

#129538 - $15.00 USD Received 3 Jun 2010; revised 3 Aug 2010; accepted 9 Aug 2010; published 3 Sep 2010
(C) 2010 OSA

in the Fig. 3) at 1.55 µm. The output power available was limited by the maximum power (1.7 W) of our pump laser. The threshold pump power as a function of ½ VCSEL temperature is shown in the inset.

The central wavelength at CW lasing operation was obtained around 1.56 µm at 0°C, with a shift to 1.57 µm at 50°C, using the maximum pump power (1.7W). The observed red shift of the central wavelength can be evaluated from the Fig. 4(a) to 0.2 nm.K^{-1}.For a constant temperature at the bottom of the gain structure and increasing pump power like in Fig. 4(b), the observed red shift of the center wavelength can be estimated to be ~ 2.9 nm.W^{-1}. These values demonstrate that this VECSEL can operate over a wide temperature range.

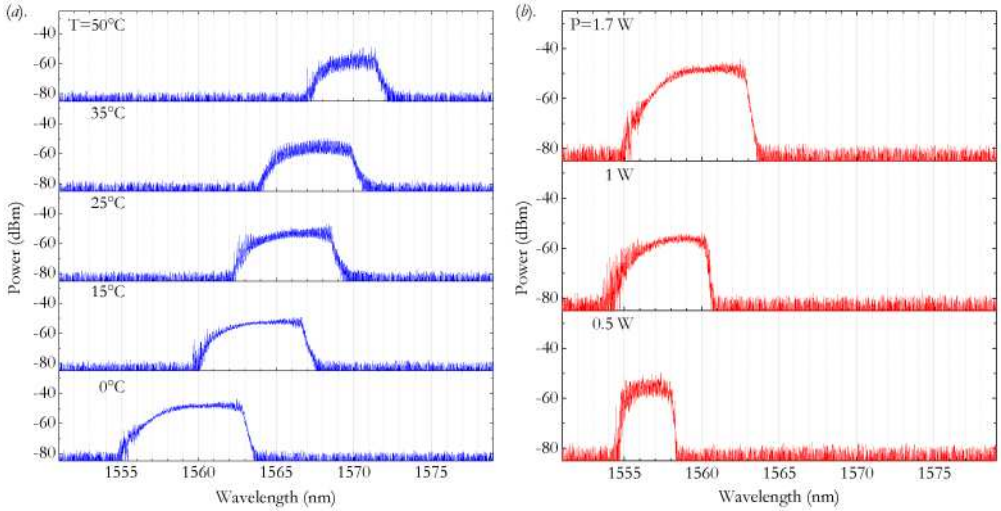

Fig. 4. (a) Optical spectra observed at different heat-sink temperatures. Pump power at 980 nm is kept at the value of 1.7 W for all measurements. The center wavelength red shift is ~0.2 nm·°C^{-1}. (b) Optical spectra observed at different pump powers. Heat-sink temperature is fixed to 0°C for all measurements. The centre wavelength red shift is ~2.9 nm·W^{-1}.

3. SESAM structure and optical characterizations

For vertical external cavity surface emitting lasers we need saturable absorbers with small saturation fluence. The absorber additionally needs to saturate faster than the gain for stable mode locking. We present here the SESAM structure in three different configurations, with the corresponding optical characterizations.

3.1 SESAM structure

The SESAM structure is grown by low-temperature (300 °C) molecular beam epitaxy. It contains, in growth order, an AlAs/GaAs Bragg mirror with 35 layer pairs over a GaAs substrate and an anti-resonant cavity incorporating a single 10-nm-thick InGaAsN quantum well surrounded by two fast recombination GaAsN layers. The GaAs cavity optical thickness has been designed to present an anti-resonant configuration in order to minimize the absorption. The absorption recovery time of the InGaAsN/GaAsN structure is expected to be around 15 ps thanks to fast tunneling and recombination into the GaAsN planes [12]. The layout of the structure is presented in the Fig. 5(a) left. The calculated reflectivity is shown on the right, together with the group delay dispersion. The GDD is in the range (-10^3 fs^2 < GDD < $+10^3$ fs^2) in the window around 1550 nm.

In order to increase the absorption in the QW, a $SiON_x$ AR layer at 1550 nm was deposited onto the SESAM surface. The Fig. 5(b) shows more absorption in the QW, the GDD becomes more flat around the region of interest as displayed on the right.

The highest absorption in the QW could be obtained using a resonant structure. We deposited a layer λ/4 of amorphous a-Si:H, with its refraction index, close to GaAs refraction

#129538 - $15.00 USD Received 3 Jun 2010; revised 3 Aug 2010; accepted 9 Aug 2010; published 3 Sep 2010
(C) 2010 OSA

index (n_{GaAs}=3.37, $n_{a\text{-}Si:H}$=3.64) [13]. This 'quasi-resonant' structure is presented on Fig. 5(c). The GDD changes rapidly in the spectral region of interest.

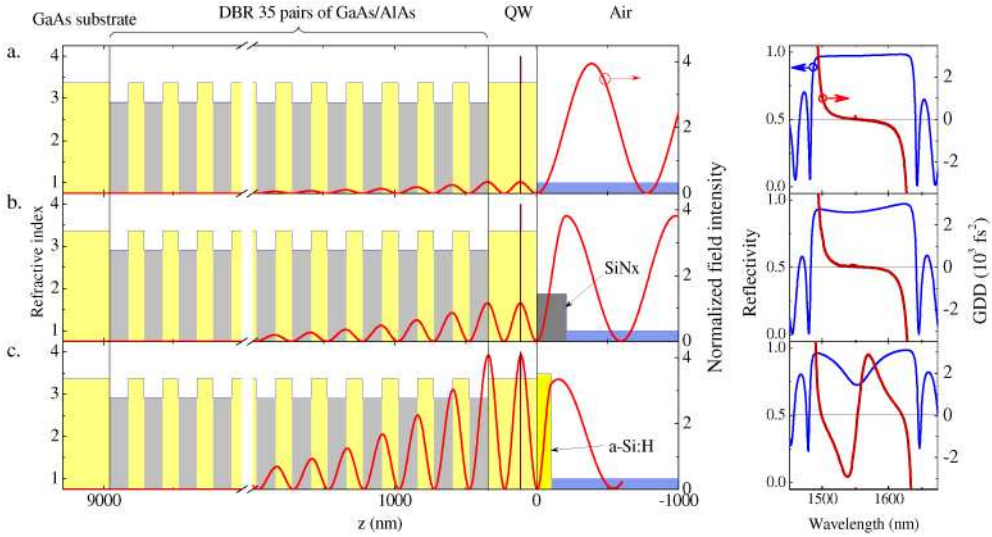

Fig. 5. Layout of the SESAM device (left) and calculated spectral properties (right) for three different cases: (a). antiresonant structure, (b). antiresonant structure with SiONx AR coating, (c). quasi-resonant structure. On the left part, the blue line represents the refractive index variations, and the red one is the calculated standing wave intensity pattern for λ=1550 nm . On the right-hand side are displayed the calculated wavelength dependence of the reflectivity (blue line) and group delay dispersion (red line).

3.2 SESAM optical characterization

The measured reflectivity spectra were close to the calculated spectra presented in Fig. 6. We describe here the nonlinear optical characteristics: nonlinear optical reflectivity, absorption recovery time. A high precision characterization setup [14] was used to measure the nonlinear optical reflectivity curve of the SESAM up to high saturation levels [15].

The SESAM nonlinear reflectivity is described essentially by the modulation depth ΔR, (the difference in reflectivity between a fully saturated and an unsaturated SESAM), the nonsaturable losses ΔR_{ns}, and the saturation fluence F_{Sat}, which is the pulse fluence (pulse energy per unit area) for which the SESAM starts to saturate. We observe a rollover at high pulse fluencies, which decreases the reflectivity after reaching a maximum value. For femtosecond pulses, this rollover is attributed to two photon absorption (TPA) in the semiconductor material [16]. This roll-over is strongly reduced in the picosecond regime [17]. The model function used to fit the measurement data is [15]:

$$R(F) = R_{ns} \frac{\ln\left[1 + \frac{R_{lin}}{R_{ns}}\left(e^{\frac{F}{F_{Sat}}} - 1\right)\right]}{\frac{F}{F_{Sat}}} \cdot e^{\frac{F}{F_2}}. \qquad (1)$$

The measurements were performed with a tunable laser source operating at a wavelength of 1550 nm. The pulse duration for the measurement was <500 fs. The different resulting reflectivity curves are shown in Fig. 6. The antiresonant structure has a small modulation depth and a high saturation fluence (Fig. 6(a)) compared to the quasi-resonant structure case (Fig. 6(c)). The antiresonant structure with AR coating (Fig 6(b)) can be considered as an intermediate between the two other structures, it has a modulation depth between the two values, and its saturation fluence equal to that for the quasi-resonant case. One notes that the

#129538 - $15.00 USD Received 3 Jun 2010; revised 3 Aug 2010; accepted 9 Aug 2010; published 3 Sep 2010
(C) 2010 OSA

quasi-resonant structure has a relatively high non-saturable loss and a more pronounced rollover at high fluence.

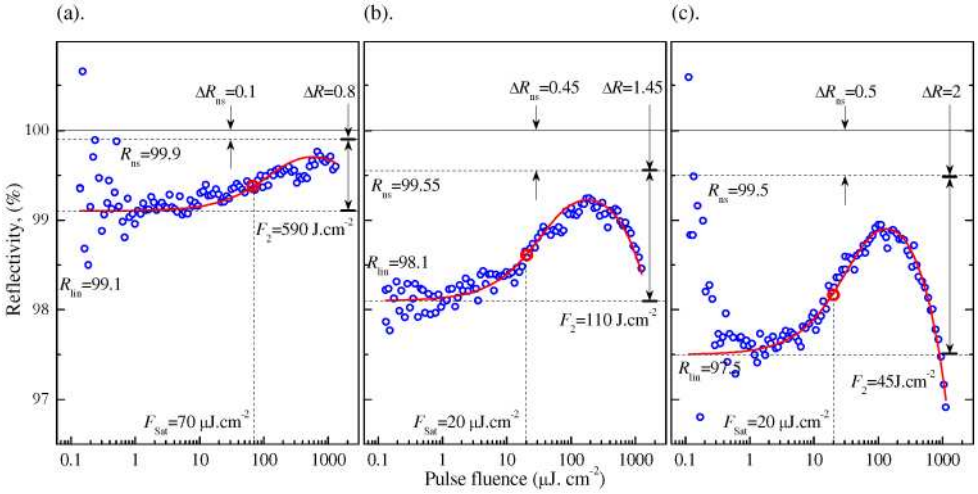

Fig. 6. Nonlinear reflectivity data for a representative sample. Blue circles: experimental data, full red line: fit-function including nonlinear induced absorption for: (a). antiresonant structure, (b). antiresonant structure with AR coating, (c). quasi-resonant structure.

The absorption recovery time was investigated by standard degenerate pump-probe experiments, in a reflection configuration, at room temperature. Measurements were performed using 150-200 fs pulses at a repetition rate of 80 MHz. The incident wavelength was set to the corresponding excitonic energy for each sample. The average beam fluence for these experiments was changed from ~20 μJ·cm^{-2} to ~325 μJ·cm^{-2}. The pump-over-probe intensity ratio was set to about 10. The reflected probe signals of all the SESAM samples could be fitted by a double-exponential decay with time constants τ_1 and τ_2. The double-exponential fit of the decay curve gives time decays of 2~3 ps for the fastest component and 25-30 ps for the slowest one. Overall, the 1/e recovery time is ~17 ps. There was not a significant difference between the behaviors of the different SESAM's structures presented in figure 6.

4. Mode-locked VECSEL performance

To achieve stable mode-locked operation, the mode area on the SESAM should be smaller than the mode area on the gain structure optimized to match the pump spot. A multi-mirror cavity enables us to obtain a control of this parameter. In the following we present the cavity configuration, the results obtained in this configuration and the optimization of the laser performance.

4.1 Cavity design

A simple schematic top-down view of the cavity is shown in Fig. 7. The configuration is an asymmetric Z-shaped laser cavity consisting of the output coupler (OC), the gain structure as a flat mirror, a folding mirror and the SESAM as an end mirror. This configuration allows for an almost independent adjustment of the mode radius on the gain structure and the absorber by varying the arm lengths [18]and a high gain where in one round trip in the cavity the beam passes twice in the gain medium and just once in the SESAM.

In the experiments described in the following, we used curved OCs with a curvature radius of R_{oc}=25 mm and 99.5% reflectivity, and a folding mirror with curvature radius R_{fold}=18 mm and with a maximum reflectivity (99.7%). The total length of the cavity is ~75 mm. The distance between the ½ VCSEL structure and the output coupler is set to ~25 mm and the distance between the SESAM structure and the folding mirror to ~11.5 mm. The

#129538 - $15.00 USD Received 3 Jun 2010; revised 3 Aug 2010; accepted 9 Aug 2010; published 3 Sep 2010
(C) 2010 OSA

calculated mode area ratio between the gain and the SESAM can reach ~25 (by slightly changing the distance between the SESAM and the folding mirror) ensuring strong saturation of the SESAM without too strong saturation of the gain. Astigmatism was kept to a minimum by keeping the angle of incidence on the spherical folding mirror smaller than 5°. The 980 nm free-space pump laser diode was positioned at a ~45° angle with respect to the ½ VCSEL.

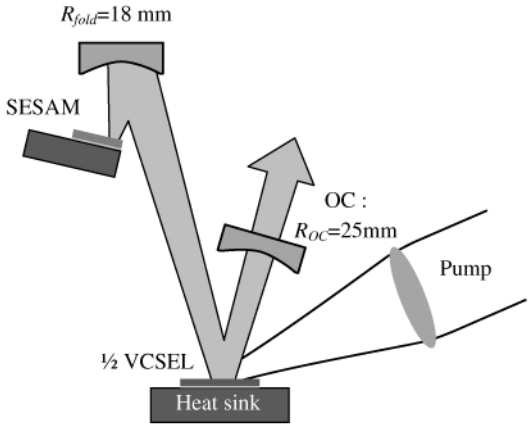

Fig. 7. Schematic drawing of the 2-GHz cavity when viewed from the top, the distance between the SESAM and the folding mirror is called ds.

Figure 8 presents the calculated values of the waist on the SESAM and the surface of the ½ VCSEL in the sagittal and tangential planes, for different cavity lengths (73, 74, and 75 mm) as a function of the distance ds between the SESAM and the folding mirror.

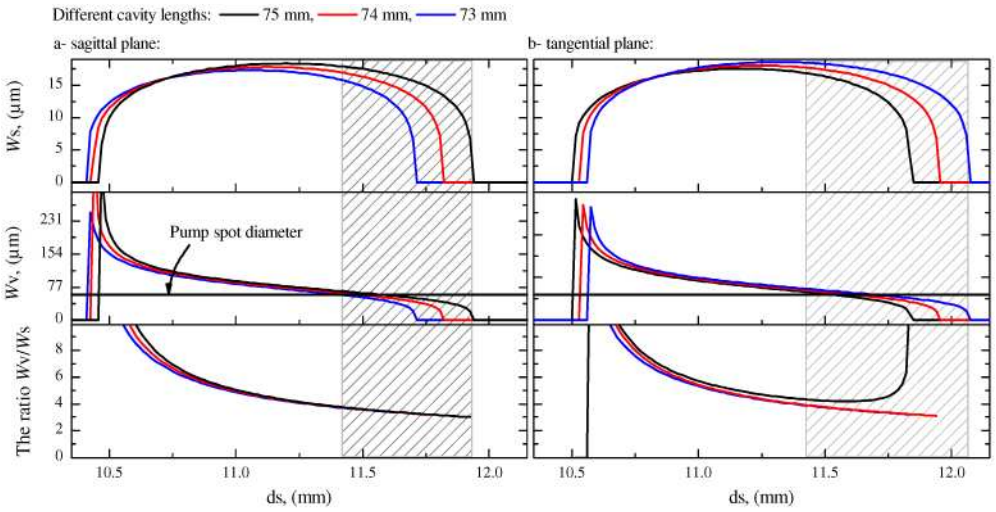

Fig. 8. Calculated values of the waists of the Gaussian mode on the SESAM (*W*s), on the ½VCSEL (*W*v), and the ratio between the two waists as a function of the distance between the SESAM and the folding mirror, for different cavity lengths, in the sagittal plane (on the right) and the tangential plane (on the left). The distance between the ½ VCSEL and the output coupler is fixed to 25 mm in all the calculations. The hatched areas are the region of laser operation.

The distance between the ½ VCSEL and the output coupler is kept to 25mm. These curves show the possibility to adjust the mode area ratio between the gain and SESAM structures through a variation of ds. This was used to control the mode-locking behavior, as is discussed in the following section 4.2.

#129538 - $15.00 USD Received 3 Jun 2010; revised 3 Aug 2010; accepted 9 Aug 2010; published 3 Sep 2010
(C) 2010 OSA

4.2 Pulse evolution

The VECSEL output was characterized using an autocorrelator, an optical spectrum analyzer, a 50 GHz bandwidth rf-spectrum analyzer with matching fast photodiode. The temperature of the heat sink was fixed at 25°C.

The mode locking was established using the antiresonant SESAM structure with $SiON_x$ AR coating (see Fig. 5(b)), because it has a modulation depth sufficient to achieve a stable mode-locking operation, in contrast to the case of the anti-resonnant structure showing a lower modulation depth (see Fig. 6b), for which no mode-locking was obtained, in spite of suitable GDD values. Mode-locking operation was also not possible with the resonant SESAM structure, having the largest modulation depth (Fig 6c), presumably due to a non-adapted GDD value (Fig. 5c).

At first, the distance between the folding mirror and the SESAM is chosen to make the calculated mode area ratio between the gain and the SESAM small (<10). The intensity autocorrelation, optical spectrum, and rf spectrum of the laser output under these conditions appear in Fig. 9(a), showing the hyperbolic secant pulse profile and asymmetric optical spectrum. The average output power in this pulse train was 56 mW, with an incident pump power of 1.7 W. We estimate the ratio of pulse fluence/saturation fluence on the SESAM to be ~0.5. The pulse duration is Δt~8.2 ps FWHM, with an optical bandwidth of 2.57 nm FWHM (central wavelength 1555 nm), corresponding to a time-bandwidth product 8.3 times above the Fourier transform-limit. The small peaks at about 5 MHz offset from the main peak at the pulse repetition rate in the rf spectrum are suppressed by more than 40 dB. We believe that residual higher-order mode beating is the proof of instability of residual pulses because they move further away or closer to the main peak depending on slight cavity length changes indicating non stability of the mode locking mechanism.

When we increase the mode area ratio between the gain and the SESAM by changing the cavity length, the intensity autocorrelation trace shows a sharp peak on top of a broader component as displayed on Fig. 9(b), while the optical spectrum shows a red shift with a slight broadening, and the position of small peaks change in the rf-spectrum, which indicates the start of single pulse formation. The measured output power decreased to 45 mW. Increasing the mode area ratio between the gain and the SESAM again makes this pulse more clear (as on Fig. 9(c)), and the rf spectrum shows two wings around the fundamental frequency.

The cavity parameter ds was continuously decreased from 9(a) to 9(e). Although it was found very difficult to know precisely by which amount between each successive adjustments, our estimate, based on the increase in RF frequency in 9(a) to 9(c), is that there was a reduction of ds by 70 µm between the settings of 9(a) to 9(c). The abrupt change in the frequency value between 9(c) and 9(d) is due to a change in the position in OC and folding mirror positions, which modified the length of the intermediate arm at this point.

If we continue to increase the gain/SESAM mode area ratio, the ultrashort pulse gets a cleaner profile as can be seen on figure 9(d) and 9(e). From the rf spectrum we can see that any small peaks around the fundamental harmonic has a direct effect on the measured pulse width. We believe that these peaks indicate a slight instability of the pulse, which can be result in a frequency chirp of the pulse (concluded from the optical spectrum). The maximum suppression of these peaks down to 55 dBm gives a pulse duration (FWHM) Δt~1.7 ps. The optical spectrum, still slightly asymmetrical, is centered at ~1562 nm and its FWHM is of ~2.29 nm corresponding to pulses with a time-bandwidth product ~1.5 times above the transform-limit. The average output power in this pulse train was 15 mW, with an incident pump power of 1.7 W. We estimate the ratio of pulse fluence/saturation fluence on the SESAM to be ~1.5.

#129538 - $15.00 USD Received 3 Jun 2010; revised 3 Aug 2010; accepted 9 Aug 2010; published 3 Sep 2010
(C) 2010 OSA

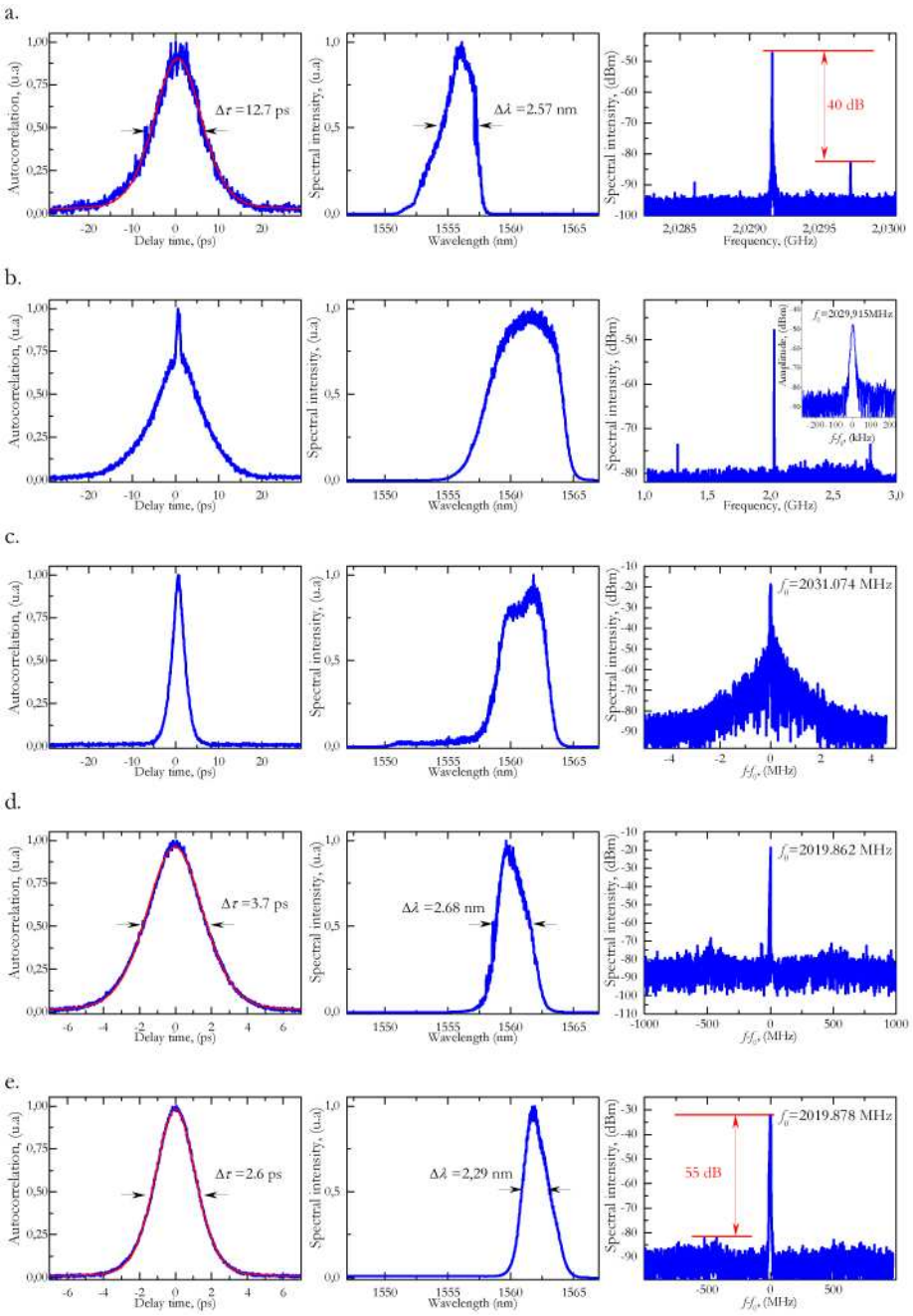

Fig. 9. Series of autocorrelation traces of pulses (left hand side), optical spectrum (in the middle) and RF spectrum of the laser output measured with a fast photodiode (right hand side), obtained from VECSEL at different settings of the cavity length, with a decreasing beam size on the SESAM surface.

The RF spectrum on Fig. 10(a) shows all harmonics limited by the bandwidth of the fast photodiode/RF spectrum analyzer combination. There is not any peak between the continuous component and the fundamental frequency as shown on Fig. 10(b). The fundamental harmonic has an estimated width at -3 dB of less than 1 kHz, using a Lorentzian fitting while

#129538 - $15.00 USD Received 3 Jun 2010; revised 3 Aug 2010; accepted 9 Aug 2010; published 3 Sep 2010
(C) 2010 OSA

it is 2 kHz for the first higher-order harmonic, as shown on Fig. 10 (c-d). This indicates that we can obtain an ultra low timing jitter from the mode locked VECSEL.

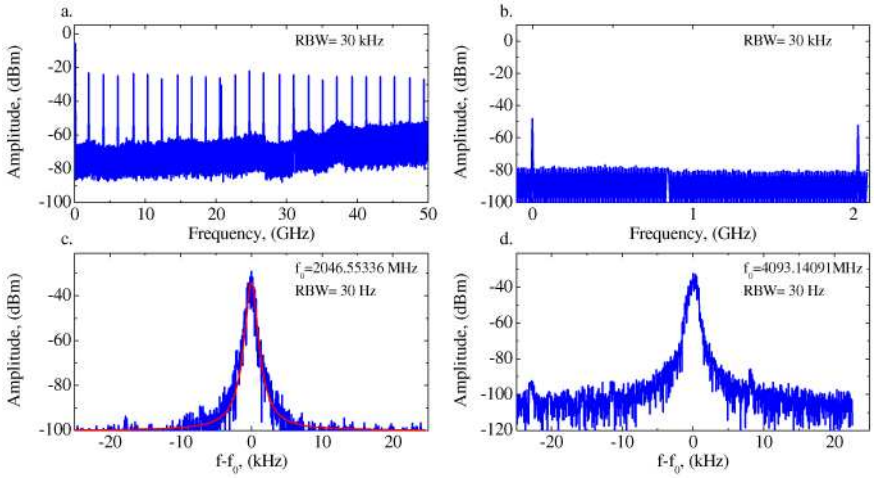

Fig. 10. RF spectrum of a fast-photodiode signal: (a). 50-GHz span and 30-kHz resolution bandwidth, the harmonics could be seen till the bandwidth limit of the fast photo diode (50GHz). (b). 2-GHz span and 30-kHz resolution bandwidth, (c). a view with a 30-Hz resolution bandwidth for the fundamental (2GHz) with a Lorentzian fit (red line) (d). first harmonic at 4GHz.

Slight variations of the pulse length, shape of the optical spectrum, and time–bandwidth product were observed over the range 0°C to 25°C, indicating small variations of the dispersion in the gain chip assembly, as presented in Fig. 11.

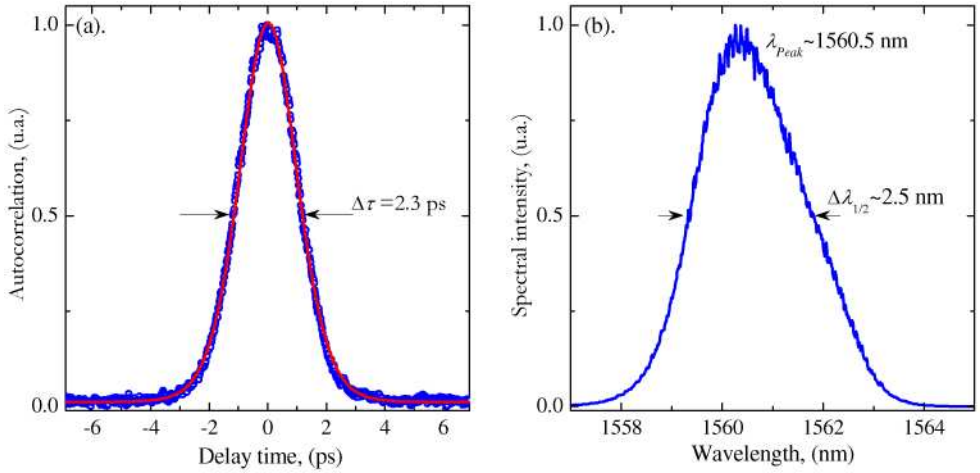

Fig. 11. Characterization of optical pulses: (a). Autocorrelation trace of the mode-locked pulses (blue points), the red solid curve represents a fit to the data assuming a hyperbolic secant autocorrelation profile with 2.3 ps FWHM at 0°C, corresponding to a pulse duration of 1.5 ps FWHM. (b). Measured spectral profile of the mode-locked laser output.

The gain effect can be studied by changing the power pumping, or changing the temperature of the gain structure. As we are limited by the maximum pump power (1.7 W), cooling to lower temperature can show the effect of gain structure, where the pulse width becomes 1.5 ps ($sech^2$ approximation), and the time-bandwidth product is of 0.46, that is ~1.4 times the transform-limit. The shift the optical spectrum towards shorter wavelength is close

#129538 - $15.00 USD Received 3 Jun 2010; revised 3 Aug 2010; accepted 9 Aug 2010; published 3 Sep 2010
(C) 2010 OSA

to the shift observed in the case of continuous mode operation of VECSEL, indicating that the performances of ½ VCSEL are dominating the whole device characteristics.

5. Conclusions and outlook

In conclusion, we have demonstrated a 1.56 µm optically pumped mode locked VECSEL at room temperature, with 1.7 ps near transform limited pulses, <1000 Hz rf-linewidth for the first harmonic, exploiting InGaAlAs/InP strained quantum well gain material and InGaAsN/GaAs quantum well SESAM material, both have been optimized for passive mode locking application.

The high gain efficiency of quaternary InP-based compounds together with the efficient heat removal from the gain structure using hybrid GaAs-based/metallic mirror combined with a CVD diamond substrate, result in a suppressed rollover in the output power. The antireflection coating added to the ½ VCSEL structure optimized with the etching of the InP layer to increase the pump absorption at 45°, to keep the resonance wavelength at 1.55 µm, result in controlled GDD from the ½ VCSEL structure, for ultrashort pulse generation.

The establishing of stable mode locking was studied from the onset, showing the effect of stable mode locking on the rf spectrum and on the form of the optical spectrum. The observed pulse width is dependent on the saturation fluence intra-cavity which should be higher than the saturation fluence of the SESAM. The current results are limited by the source pump power. With further higher pumping powers (and fine adjustment of the spectral and GDD characteristics of the SESAM and ½-VCSEL elements), we expect to scale down the pulse width below 1 ps. Further studies are necessary in order to improve the pulse width and the timing jitter in the passive mode-locking regime, at higher output powers.

Acknowledgments

Dr Juliette Mangeney, IEF, Orsay, France and Dr Yohan Barbarin in the group of Prof. Ursula Keller, ETH, Zürich, Switzerland are gratefully acknowledged for the help in SESAM characterization. This work was partly supported by Agence Nationale de la Recherche (ANR-TONICS project), and the European Network of Excellence 'ePIXnet'.

#129538 - $15.00 USD Received 3 Jun 2010; revised 3 Aug 2010; accepted 9 Aug 2010; published 3 Sep 2010
(C) 2010 OSA